Chapter 5

Temperature measurements

5.1 Particle velocity and energy

In this chapter we will discuss measurements of the electron energy distribution function of the plasma. By taking the first moment of this energy distribution we arrive at the average thermal energy of the electron population, which is proportional to the electron temperature of the plasma for a Maxwellian equilibrium, $\langle E_{thermal} \rangle = \frac{1}{2} n K T_e$. Here n is the number of degrees of freedom that the plasma electrons can move in, which is 3 for our system, and $K = 1.38 \times 10^{-23}$J/°K is Boltzmann's constant, and so KT has units of energy. Because the electron and ion populations are distinct interpenetrating fluids, it is possible for them to not be in thermal equilibrium with each other and exist with different energy distribution functions, and different temperatures.

When thinking about the kinetic energy of the plasma particles it is important to distinguish between their drift and thermal velocity components. The drift velocity of the plasma is defined to be the average velocity of all the particles with a macroscopic fluid element, relative to the rest frame of the laboratory. In other words, the drift velocity is the fluid flow velocity of the plasma. It may vary with position, since the fluid elements may be flowing along the streamlines of some non-uniform velocity field.

In the CTIX accelerator, the plasma drift velocity is dominantly in the direction of the axial acceleration, although there may be some smaller toroidal or poloidal component of the velocity of individual fluid elements. On the largest scale however, if we average over all the particles in a thick annular slice at a given axial position, any poloidal rotation of the fluid will average to zero over the cross section, while toroidal rotations may exist but are expected to be much smaller than the dominant axial velocity. This is what we often call the CT velocity, and it is what we can measure with time-of-flight analysis of sequential magnetic probe signals, or with Doppler spectroscopy under certain conditions.

On the other hand, the thermal velocity component of any particle is simply the velocity vector that remains when we subtract the drift velocity from the particle's velocity relative to the lab frame. In this way, a particle's velocity vector is the vector sum of its thermal velocity component, and the drift velocity of the fluid.

$$\mathbf{v}_{particle} = \mathbf{v}_{drift} + \mathbf{v}_{thermal}$$

This thermal velocity will vary randomly in direction and magnitude as we go from particle to particle. We can characterize this random variation by the distribution function of the thermal velocity. We will also separately take account of the drift energy, and the thermal energy of each particle,

$$E_{drift} = \frac{1}{2} m v_{drift}^2 \ , \qquad E_{thermal} = \frac{1}{2} m v_{thermal}^2$$

where m is the mass of the particle.

5.2 Thermalization of electrons

A thermalization effect occurs when a compact toroid is injected into the vacuum magnetic field of the Davis Diverted Torus. Experiments were conducted in which the CT was injected transversely ($\perp$) into magnetic fields of 105, 150, and 180 Gauss, each defining a distinct data set. Due simply to the net motion of the CT the ions have a drift kinetic energy in the range of 100 eV

to 200 eV. The electrons, in contrast, gain little kinetic energy from the net motion of the plasma, owing to their much smaller mass (1/1856 of the mass of a proton); the net drift contributes no more than 0.1 eV to the electrons, which is insignificant compared to the electron thermal energy of 10 eV or greater.

During the process of collision and reconnection with the magnetic field of DDT the initial velocity field cannot stay directed axially. As the center of mass of the CT is brought to rest the original directed kinetic energy is converted into thermal energy as the anisotropy of the particle velocity field is lost to a more isotropic velocity field in which entropy is maximized. While this basic concept provides a general description of thermalization, it leaves many questions unanswered. A more complete and predictive model would need to delineate the mechanisms that enable the conversion of particle energy to field energy and vice versa, as well as coupling between particles, such as the energy transfer from the ions to the electrons. These mechanisms could include kinetic effects, possibly via collisions, wave growth instabilities, and kinetic damping. Fluid effects could also be important, such as a turbulent cascade of fluid energy down to microscopic dissipative scales, shock heating, and magnetic reconnection. The theory behind these issues is far too extensive to tackle within this dissertation. However, the basics can be outlined, and several new experimental findings can be reported, which may help future work toward confirming existing theories, or guiding the invention of better theories.

The fundamental concept needed to describe the process of thermalization is the distribution function of the thermal energy of the particles; we will notate the energy distribution by $f_E(E)$. The energy distribution function $f_E(E)$ expresses the electron population density as a function of energy. If it is normalized to unity (the convention that I usually prefer), then $f_E(E)$ also represents the probability that any single electron will be found to have a thermal energy in the neighborhood of the energy E.

And of course there are other relevant particle distribution functions. For example $f_E(E)$ is related to the speed distribution by $f_E(E) = Jf_v(v(E))$ where v is the speed, or magnitude of

the velocity of a particle, and J is the Jacobian of the transformation $v \rightarrow E(v) = \frac{1}{2}mv^2$. Then $J = |dv(E)/dE| = |(2mE)^{-1/2}|$.

For reference purposes I would like to include some relevant formulas here. The velocity distribution function for a Maxwellian equilibrium of temperature T, with n spatial degrees of freedom, normalized to unity is

$$f(\mathbf{v}) = \left(\frac{m}{2\pi KT}\right)^{\frac{n}{2}} e^{-\frac{m|\mathbf{v}|^2}{2KT}} \tag{5.1}$$

where the n components of $\mathbf{v}$ range over the domain from $-\infty$ to ∞.Although the velocity distribution depends only on the speed $v = |\mathbf{v}|$, it is critical to remember that the distribution function for the speed v of a particle, ie the speed distribution, is not the same as the velocity distribution. The Maxwellian speed distribution function in the case of $n = 3$ is

$$f_v(v) = \frac{4}{\sqrt{\pi}} \left(\frac{m}{2KT}\right)^{\frac{3}{2}} v^2 \; e^{-\frac{mv^2}{2KT}} \tag{5.2}$$

where the domain of $f_v(v)$ is $0 \leq v < \infty$.From the speed distribution we can write down the energy distribution function for a Maxwellian system ($n = 3$),

$$f_E(E) = 4\pi^{-\frac{1}{2}}(KT)^{-\frac{3}{2}} m^2 \; \sqrt{E} \; e^{-\frac{E}{KT}} \tag{5.3}$$

where the energy is, of course, always positive; $0 \leq E < \infty$.

On the CTIX device, we have successfully measured electron energy using a pair of electrostatic energy analyzers. We found that immediately before the collision/reconnection the electron thermal energy was approximately 30 eV to 40 eV and afterward the thermal energy increases to greater than 70 eV. Ion thermal energy is also expected to increase during the collision, however experimental verification of this effect remains incomplete. An attempt was made to repeat the energy measurement on the ion population using a larger 4-grid Ion Analyzer Probe. This was ultimately not successful. The measurement of ion thermal energy is more challenging due to the larger diameter ion Larmor orbits and certain plasma sheath effects.

A Note on Distribution Functions A quick comment should be included here regarding a difference of terminology. The function that physicists call a distribution function (as I have been using it above), is the same thing that mathematicians somewhat more precisely refer to as a probability density function (or pdf). The math nomenclature does a better job of conveying the meaning of the function because the integral of a pdf over a given interval results in the probability that the continuous random variable will take on a value within the limits of integration. In this way the value of the pdf at any given point represents the density of probability of random occurrence near that point. It reminds us that we need to integrate the pdf to get a value that is actually a probability. To add to this confusion, mathematicians have given the name 'distribution function' yet another definition, F(X) which is the integral from $-\infty$ to X of the pdf f(x). The mathematician's distribution function measures the probability of the event that the random variable will take on a value less than X. This will never be what I mean when I refer to the distribution function of some variable. I will always use 'distribution function' as the physicists do, equating it with the mathematician's pdf. And since my audience is primarily composed of physicists, I will follow their convention and mainly speak in terms of distribution functions.

5.3 Experimental Overview

In our experiments we measured the electron energy distribution before and after it interacts with the DDT target magnetic field using electrostatic energy analyzer probes (EAP) in a variety of configurations. For all of these experiments we measured the initial velocity of the CT as it entered the injection region, as well as the final velocity of the reconnected plasma as it propagated along the field lines of DDT.

We wanted to know how the initial and final states scale with injection energy, and so we repeated the same measurements for three different accelerator settings, CTIX accelerator voltage at 9.5 kV, 12 kV, and 15 kV. For this sequence of data sets, we adjusted the strength of the tokamak

field to follow the increased accelerator voltage,(B_{DDT} = 105, 150, and 180 G). We did this with the intention of maintaining the CT stopping condition. As we will see, because of some accelerator inefficiency, the CT injection velocity did not depend on V_{acc} according to a simple, monotonically increasing function, like we naively expected. Instead, the velocity peaked near 12 kV, and then fell off as the applied accelerator voltage was further increased. The result is that we explored a much broader variety of stopping conditions than we originally planned. [tabulate stopping parameters for the three settings, to show that 9.5 kV data set should not have been stopped by the field] The details of the design and operation of gridded electrostatic energy analyzer probes is presented below, which includes an analysis of simulated data to arrive at an estimate of the experimental error, as well as some statistical results regarding the systematic error due to the analysis algorithm.

5.4 EAP Construction

The probe tip is a hollow cylindrical assembly, 2 cm in diameter, made from anodized aluminum with a moderately large 1 cm diameter aperture to let plasma inside. Within the probe tip are the following components: two circular grids, (the ion repeller grid and control grid), and a circular collector plate. They are stacked together in a sandwich configuration with mica spacers to insulate them from each other and from the case of the probe tip. The probe tip is supported by a 28" long stainless steel shaft which slides through an o-ring vacuum seal to allow the probe to be inserted into the vacuum vessel over a range of depths.

The two grids are tungsten mesh of high transparency, and the collector is tantalum. The two grids and the collector each have a thin nickel wire spot-welded to them that runs back through the shaft and connects to the electronics that operate the probe. By way of these wires the grids can be charged to different potentials and a current can be drawn from the collector plate, and recorded by a digitizer. We will ultimately derive the electron energy distribution function from measurements of how the electron current drawn by the collector plate depends on the applied repeller grid voltage.

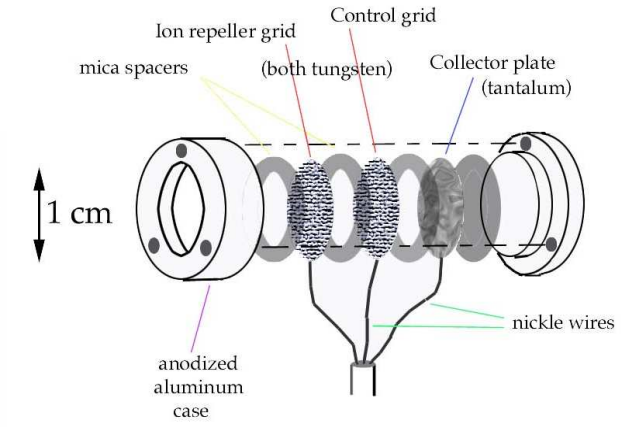

Figure 5.1: Exploded view of EAP showing grids and collector plate

For our experiments the energy analyzer probe tip was positioned at the center of the vacuum vessel with the aperture oriented toward the incoming plasma to have the best opportunity to intercept a good signal. For the injection experiments involving collision/reconnection on DDT target field,the EAP was mounted on the top port 90^o from the injection point on DDT, then for the pre-injection measurements, the probe was positioned in the drift section.

5.5 Grid biasing

The functionality of the energy analyzer probe, is achieved primarily by charging the control grid to a negative potential with respect to ground. This potential on a probe is often referred to as the bias voltage or simply the bias. Negatively charged electrons that initially enter the aperture of the probe will feel a repulsive force from this grid. The electric field of the control grid can be thought of as an electrostatic hill standing between the electrons in plasma and the collector plate. This hill will act to separate those electrons which are fast enough to make it over the hill from those which are too slow to get over the hill. All of the electrons that do make it over this hill are

then promptly absorbed into the metal collector plate, causing an AC-coupled negative current to flow across a bias capacitor and then back to the digitizer.

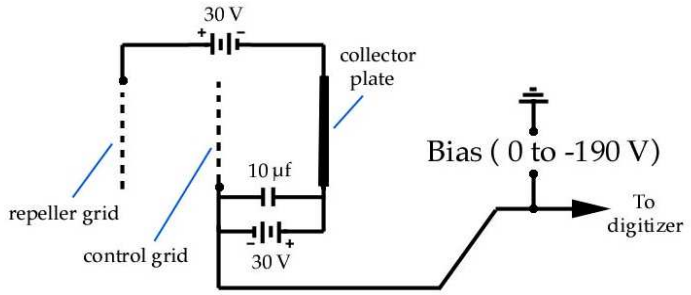

Figure 5.2: Schematic of EAP biasing circuit

The magnitude of this current is directly proportional the total number electrons in the vicinity of the probe which had enough energy to make it over the hill. In Fig. 5.3 we have shown the collector current as a function of time over the course of a typical shot.

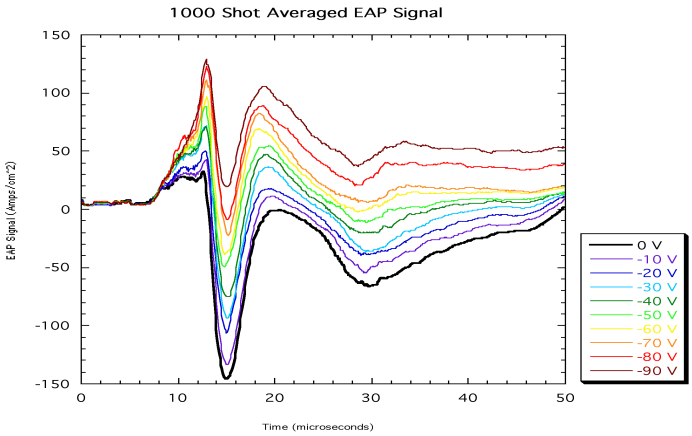

Figure 5.3: Time dependence EAP collector current, parameterized by control bias voltage. As the negative bias is increased a larger electron fraction is repelled.The first strong negative peak in the signal corresponds to the arrival time of the compact toroid.

Now, as we vary the bias voltage applied to the control grid we will repel a variable amount

of electrons, in a manner that is energy dependent. At a larger negative bias,more electrons are repelled by the control grid, letting only the very fastest electrons get to the collector plate, hence a small current is drawn. When we decrease the magnitude of the bias, very few electrons are repelled hence a very large current. At zero bias, all the electrons can get by and so the current has leveled off to a maximum value.

The other grid in the probe, the ion repeller grid, is situated to be the first to encounter incoming plasma and is charged positive in order to prevent ions from entering the interior of the probe. In the simplest possible biasing circuit, the positive bias on the ion repeller grid is accomplished using a high impedance battery, that provides a DC voltage yet blocks the fast signals caused by interaction with the transient plasma.

5.6 Relation between $I(V)$ and $f_E(E)$

Everything that I have already described about the operational mechanism of the EAP, and how it can be used to measure the electron temperature of a plasma can be succinctly summarized in the following integral relationship between $I(V)$ and $f_E(E)$. Because the electron energy distribution $f_E(E)$ measures the probability density of electrons in each infinitesimal slice of energy space, we can express the collector current $I(V)$ as an integral of the electron energy distribution.

$$I(V) = q \cdot \Gamma \int_{qV}^{\infty} f_E(E) dE \tag{5.4}$$

Here, q is the charge of an electron, it works as the conversion factor between V in Volts and E in electron-Volts. This integral counts all of the electrons which have an energy above (qV), which are collected as electron current by the EAP when the bias voltage is V. Randomness enters our measurements primarily from the electron flux rate $\Gamma = n_e v_e A_{collector}$ which varies from shot to shot with an approximately Gauss-normal distribution. Here n_e is the electron number density, v_e is the average electron speed (dominated by thermal motion), and $A_{collector}$ is the area of the collector plate. The physical source of this variation is mostly due to irreproducibility in the total gas output

of the formation gas valve, and also partly due to spatial variations in plasma density and how that density intercepts the probe. Now, it is the current that is experimentally measured, initially as the set of data points making up the I-V scatter plot, one (I, V) point per CTIX shot.We first need to extract an approximate the function $I(V)$ from the raw data by some averaging or curve fitting procedure.Once we have the measured $I(V)$, we can solve equation 5.4 for the unknown $f_E(E)$ by differentiating both sides.

$$f_E(E) = \frac{1}{q\Gamma}\frac{dI(V)}{dV}\bigg|_{\frac{E}{q}} \tag{5.5}$$

We also see that $V = E/q$ is the bias voltage which is able to repel an electron of energy E.

Lastly, the average thermal energy is computed by taking the first moment of the energy distribution function.

$$\langle E_{thermal} \rangle = \int_0^\infty E f_E(E) dE$$

So the experimental task is to find a feasible way to measure the I-V curve with the EAP so that we can differentiate it to get the local electron energy distribution function. In our setup we do not try to measure the energy distribution of the plasma for each individual shot because the desired plasma conditions in the vicinity of EAP are so transient. The plasma wave passes over the probe for only a few microseconds and then is gone. While it is physically possible to sweep the bias over a few hundred volts at a MHz rate, we believe that the cost and inherent difficulties in implementing and operating such a system would overshadow any benefits for measuring the fast plasmas on our experiment.

It is more experimentally feasible to build up the I-V curve point by point, one point for each shot. To make this pointalistic composite of the I-V curve we collected 20 shots per bias voltage setting, with a total of 20 settings from 0 volts to -190 volts in increments of -10 volts. This gave a total of 400 shots per data set in the original post-reconnection measurement of electron temperature.

We were careful not to take all 20 shots for a single bias voltage at once. We broke up the bias settings into even and odd multiples of -10 V. We would first go sequentially through the even

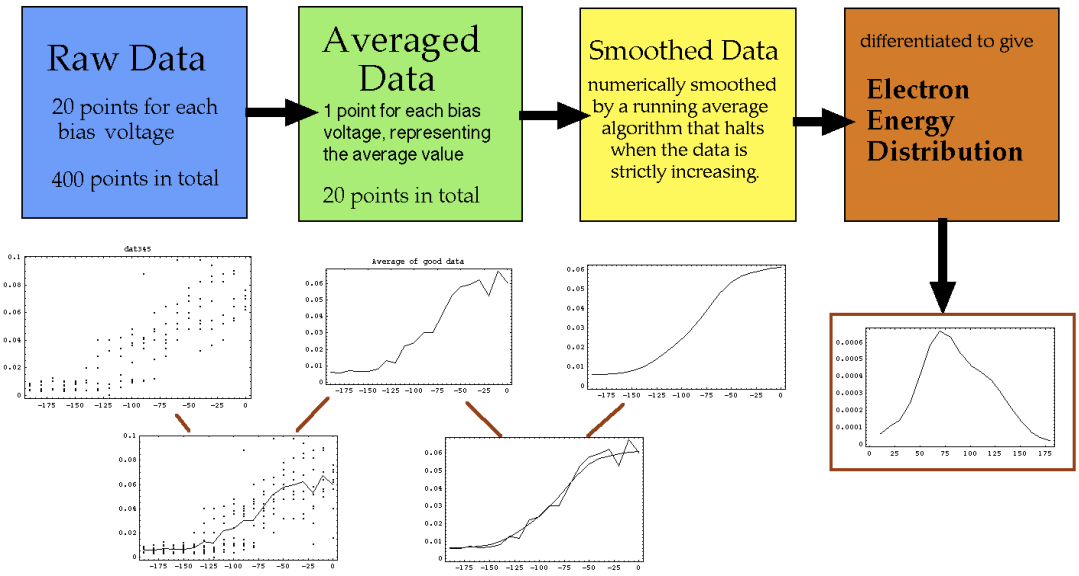

Figure 5.4: Analysis method using moving-window smoothing

set, with 10 shots at each setting, then do a round on the odd set with 10 shots per bias setting. Then we repeat this to get the second 200 out of 400.

The reason for dividing the scan into a several repetitive cycles was to separate out any systematic trends in system performance from the real electron temperature effect. For example, it might be a problem if all the low bias voltage shots we taken at the beginning of the day, and all the high voltage shots at the end of the day. There would no way of knowing that as the device warmed up over the course of the day, variation in the gain of the electronics or in the performance of the accelerator was the real source of the observed trends in the data.Based on the comparison of these divided data sets, we found that there was no measurable systematic variation in the performance of the EAP diagnostic over the course of several weeks of runtime.

5.7 Analysis Methods

Method 1: Two Parameter Nonlinear Fit to a Maxwellian form I(V) Curve. Assumes that plasma is in thermal equilibrium with an effective number of degrees of freedom that must be chosen by the user. Program returns a Temperature and a Normalization FactorThe idea is that if the electrons had a Maxwellian distribution, then the $I(V)$ curve for the EAP should obey some analytically expressible formula. If we evaluate equation 5.4using the Mawellian energy distribution given in 5.3, then we find

$$I_{Maxwell}(V) = 1 + \frac{4}{\sqrt{\pi}} m^2 \sqrt{\frac{qV}{KT}} e^{-\frac{qV}{KT}} - Erf\left(\sqrt{\frac{qV}{KT}}\right) \tag{5.6}$$

Method 2: Non-analytical Free Fitting Method. Using no analytical assumptions about the form of the Energy Distribution Function, this method is able to reconstruct deviations from thermal equilibrium that may exist within the plasma. The Raw Data is averaged, smoothed and then differentiated numerically to yield a discretized plot of the Energy Distribution Function.Both Methods have been implemented and compared.

5.8 Experimental results

graphs (f(E), and velocity histograms, for each DS) with a few comments, and a table

Each of the 10 colored line-plots in the 1000 shot Average is the point-by-point time-dependent average of the 100 shots that were all taken at the same Bias Voltage.On the right are individual EAP signals for two shots that contributed to the 1000-shot average graph. The important features here are first, the strong negative peak that occurs at the time of SCT arrival, and second, the weaker negative pulse that is due to the Trailing Plasma eventually getting to the probe. The top signal was taken with Electron Repeller Bias Voltage set to zero and you can see that both the

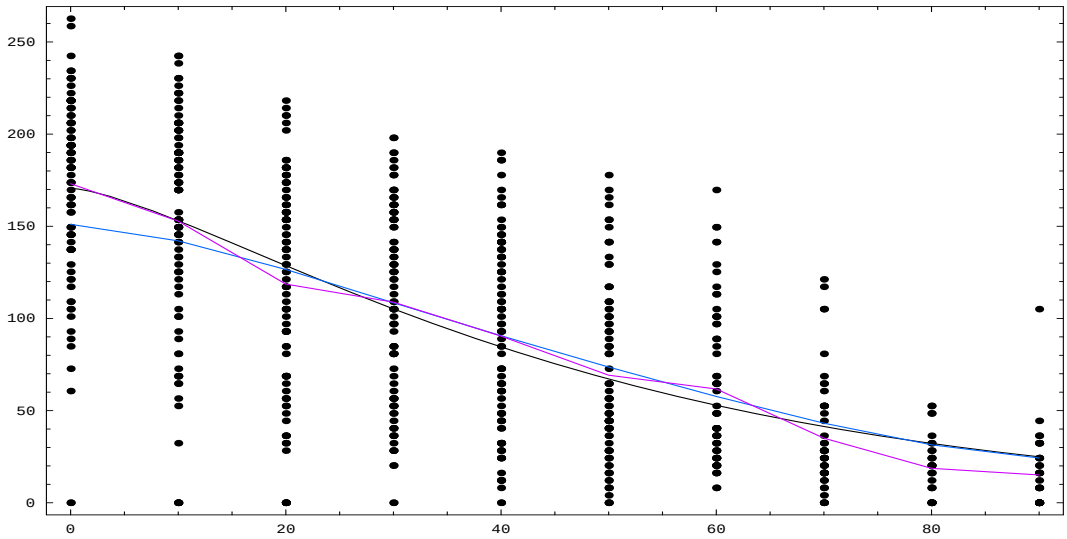

Figure 5.5: Raw data {•} with average-value curve {violet}, iteratively smoothed curve {black}, and Maxwellian fitted I-V curve {blue}.The x-axis measures the absolute value of the EAP bias voltage, and the y-axis measures the resulting EAP collector current (arbitrary scale).

Table 5.1: Summary of results from 9.5 kV data set

$\mathbf{V_{acc} = 9.5\ kV}$, $\mathbf{B_{DDT} = 105\ G}$	*Pre-injection*	*Post-reconnection*
Fluid velocity	13.65 $cm/\mu s$	5.95 $cm/\mu s$
Net Ion Kinetic Energy	97.2 eV	18.5 eV
Electron Thermal Energy	unknown	70.1 eV

Table 5.2: Summary of results from 12 kV data set

$\mathbf{V_{acc} = 12\ kV}$, $\mathbf{B_{DDT} = 150\ G}$	*Pre-injection*	*Post-reconnection*
Fluid velocity	18.4 $cm/\mu s$	14.95 $cm/\mu s$
Net Ion Kinetic Energy	176.7 eV	116.6 eV
Electron Thermal Energy	unknown	86.4 eV

Table 5.3: Summary of results from 15 kV data set

$\mathbf{V_{acc} = 15\ kV}$, $\mathbf{B_{DDT} = 180\ G}$	*Pre-injection*	*Post-reconnection*
Fluid velocity	12.14 $cm/\mu s$	10.26 $cm/\mu s$
Net Ion Kinetic Energy	76.9 eV	54.9 eV
Electron Thermal Energy	unknown	80.3 eV

SCT and the Trailing Plasma cause electron current to be collected by the probe. When we increase bias voltage to the -90 V in this lower shot, it is clear that almost all electrons have been repelled.

Pre-injection electron measurements Method 1: Maxwellian Fit Average Thermal Energy = 33.47 eV Errors are unknown

Method 2: Free Fit Average Thermal Energy = 43 eV The Error due to Data Set Size and Quality is $\sigma^2_{Thermal\ Energy} = \pm 2.02788\ eV$ The Error due to Smoothing is s2Smoothing = ± 2 eV

5.9 Error analysis of simulated data

We shall closely examine two cases, one simulation done on with a Maxwellian input distribution and one done with non-Maxwellian input distribution. Here is the Maxwellian energy distribution. [figure ?]It has an average thermal energy of 1.4 (arbitrary units). We integrate this analytically to create the ideal I-V curve, from which we can generate a simulated data set which constitutes the "measured" I-V curve. This is shown below.

This data has 400 points in it, just like a real data set. To make the points scatter, for each bias setting, we generate 20 normal-random numbers from 0 to 2 which have the same standard deviation as the real data set does and we use these numbers as the vertical distance of the data points away from the ideal I-V curve. To do this we just multiplied the 20 normal-random numbers by the height of the ideal I-V curve to get the scatter of points in right relative frame above and below the ideal curve.

If the input and output distributions were wildly different in the simulation, then we would expect that the experimentally measured distribution would also be wildly different from the idealized, physically real distribution. If the input and output distributions were very similar, and this similarity held for a wide range of input curves then we would be guaranteed an equivalent level of similarity between our measured energy distribution and the actual energy distribution of the plasma We then accept the simulated data as being "real" and do our analysis on it.

Below is the energy distribution reconstructed from the data. It has close to the same average thermal energy of 1.44 which differs from the average value of the original by about 3%.

The distribution's shape has spread out quite a bit due to the effects of randomization in creating the simulated data. This is not an error in the average, smooth, differentiate algorithm because when simulations were done with 2000 data points in the set, we reconstructed the proper shape of the distribution quite well.

As the number of data points shrinks, the reconstructed distribution become correspondingly more squashed out. This spreading is due primarily to our data size of 400 points. In addition, different randomizations produced slightly different data sets, and hence slightly different reconstructed energy distributions. This kind of fluctuation was examined informally, and it was observed to be relatively small in the Maxwellian case with 400 points. No simulated sets produced humps where they were none to begin with.

In this way all of the Maxwellian reconstructions were easily identified as being Maxwellian. For comparison, we tried using a non-Maxwellian distribution as the input for the simulation. Here we have the original distribution, its average thermal energy is 3.3. Using the same simulation algorithm as before, we create the "measured" I-V data set as shown below. We then try to reconstruct from this data set and yield the reconstructed energy distribution. While its shape is quite different from the original, its average thermal energy is still very close, 3.46 which is within 4.8% of the original. Many other functional forms were tried as the input for the simulation. Similar results were obtained for all simulations using the same statistics as our actual data sets. In all but a few of these runs, the average value of thermal energy was correctly reconstructed to within 5% of the original.

5.10 Statistical error analysis

The main result from the simulation work was that the average value of thermal energy had a relatively small total error for the size of data sets we are working with. In this section we take this result a step further by deriving exact an relationship between the data set dimensions and

the resulting error in the average thermal energy of the plasma.

We consider a situation where the probe current $I(V)$ has been measured n_V times at the k bias voltage settings, where in general, n_V could take different values at different bias voltages, hence the V index is used to denote this possible dependence. A non-constant n_V could easily occur in a real life experimental data set, where system failures of one sort or another could require that data from certain shots be excluded from the dataset. The result would be a slightly patchy scan of the parameter space,where more good data was gathered for some voltage settings than for others.

[figure I-V raw data, caption: n_V samples of probe current k bias voltage settings]

To get the Energy Distribution the data is averaged, smoothed until it is a well-behaved monotonic function, and finally differentiated to yield the Energy Distribution.

[figure]I-V raw data Average Data Smooth Data Energy Distr.

For now, will ignore the smoothing step, which only acts to decrease the error by bringing the data closer to the real distribution. Without the smoothing step we will be looking at upper bounds for the errors involved with this sampling process. The variable Γ was observed to be normally distributed about the mean density.

Because each $I(V)$ measurement depends on the random variable Γ and a monotonic function of V, the variance of the I data at V obeys

$$\sigma^2(V) = \sigma^2(0) \cdot \int_{qV}^{\infty} f_E(E) dE \tag{5.7}$$

Note that the variance at $V = 0$ should be equivalent to variance that describes how the electron flux rate Γ is randomly distributed, ie $\sigma^2(0) \equiv \sigma_\Gamma^2$.

As mentioned earlier, the random variation in $I(V)$ is due almost entirely to fluctuations in Γ, while the stable dependence on voltage is due entirely to the integral of $f_E(E)$, and so the variance will decrease with increasing $|V|$.

This is condition is useful as an indicator of whether or not the probe is really working. If $\sigma^2(V)$ doesn't decrease then there is a problem with the probe. Error bars for the values of the

$I(V)$ curve at each voltage can then be estimated from the measured $\sigma^2(V)$ and the number of data points n_V at that energy. For each voltage setting, the variance of the of average value of the (n_V) probe current measurements is related to the variance of the measurements themselves, according to

$$\sigma^2_{ave}(V) = \frac{\sigma^2(V)}{n_V} \tag{5.8}$$

Of more importance to this study is an upper bound on the error of the average thermal energy, quantified by the variance first moment of $f_E(E)$. We used moment generating functions to make the transformation from the variances of the individual measurements to the variance of the error in the average thermal energy. The resulting total variance is just the sum of the variances of the average value at each voltage $V_1, V_2, \ldots, V_k$.

$$\sigma^2_{thermal\ error} = \frac{\sigma^2(V_1)}{n_{V_1}} + \frac{\sigma^2(V_2)}{n_{V_2}} + \cdots + \frac{\sigma^2(V_k)}{n_{V_k}} \tag{5.9}$$

The key feature in this expression is that the error will tend to grow linearly with k, ie the number of bias voltage settings in the scan(also the number of terms in this sum). It must be noted that it does not work to try to minimize the error by taking k =1, since your choice of that single voltage setting will dominate the final answer. Enough voltage settings must be included in order to have a minimum amount of energy resolution to consider the final result a reasonable approximation to the distribution function. With that in mind, k should be at least 10, and then n must be chosen to be large enough to bring down the error. (k =10, n=200 are good values to plan an experiment around).

5.11 Effect of smoothing

5.12 Summary of results

The simulation has shown the limitation of accuracy of our experimental method when only 400 data points are taken. The exact shape of the distribution can not be trusted, except that

if it has some lumps in it is very unlikely to be from a Maxwellian plasma. If is has no lumps, the physically real energy distribution still has a chance of being non-Maxwellian. On the other hand we can put more confidence in the average thermal energy of the distribution.

The simulation has shown that our analysis on 400 data points is fairly robust with respect to this average value, and we can expect that with our real data we have correctly reconstructed the average thermal energy of the plasma to within 5%.

When we compare the results of the EAP study to the results of Time of Flight study we find that the final electron thermal energy is comparable to final ion kinetic energy. This implies that electrons and ions have gone through some process of equilibration during the collision.

We notice that of the three data sets gathered in this study, the 15 kV and 12 kV sets have similar, non-Maxwellian energy distributions as well as post-collision loss of net flow velocity. The 9.5 kV set had a much greater loss of flow velocity and in addition appeared to have a more Maxwellian shaped distribution. This supports the model that in the 9.5 situation the interaction of the CT with the DDT field results in the plasma coming to a dead stop at the point of injection and then slowly diffusing out into DDT.

Where as with the 12 and 15 sets, a definite post collision plasma wave propagates through the vacuum field of DDT carrying significant mass and kinetic energy. The primary variable which must be used to account for this difference are gun velocity and DDT field strength. For 12 and 15 the field strength was 150 Gauss and 180 Gauss, respectively. For the 9.5 set the field was only 105 Gauss, yet the gun velocity was higher than for the 15 data set. This could indicate that in 9.5 case the field was not sufficiently strong to capture the CT before it collided with the back wall of the DDT vacuum vessel. If CT-wall collision occurred then the post collision plasma would likely have completely different thermal properties.